Image Fix Model for Belt Fusing System

David Battat, Lexmark International, Lexington KY

Abstract

A first principle formalism is proposed for image fix to describe Taber abrasion as well as crease in a hot roll belt system, which takes into account the conditions in the nip as well as the media thickness and backup roll temperature. First order explicit relationships are derived for fuse grade performance, which agree with existing predictions and measurements. The analysis can be used to design the fusing process and select materials and hardware.

Image Fix

In instant-on belt fusing, the system uses the heat generated by the heater more or less as it is generated, as there is no metal core with stored thermal energy. In this case, the temperature of the backup roll and the thickness of the media become important and can have a bearing on belt temperature and heat management. The temperature of the backup roll depends on initial warm-up time and, more so, on the inter-document gap and transient operation. In the present paper, a first principle formalism is proposed for image fix, that takes into account backup roll temperature and media thickness.

Figure 1 illustrates the fusing system addressed in the present paper.

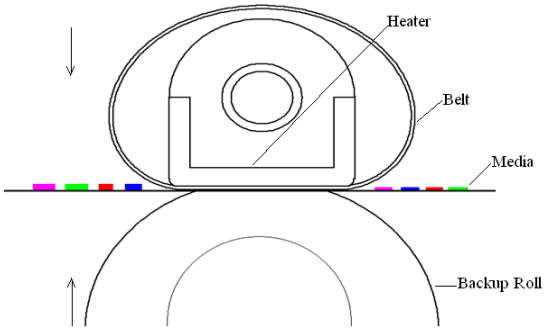

***Figure 1**. Instant-on Belt Fusing*

The primary function of a fuser is to fix the toner images to paper, and to do this satisfactorily throughout the design life of the fuser. Modeling image fix is needed to shed light on the underlying physics, and also to help design the fusing process, which in turn dictates hardware and material selection. Fix phenomenon is too complex to be amenable to a fine analytical description. The difficulty is further compounded by the fact that fix performance is judged by methods such as Abrasion, Crease, and Tape lift-off, that are not mechanistically equivalent. Likewise, an empirical model derived from testing a specific hardware is of limited use.

Image fusing is primarily controlled by toner rheology and by paper properties. Toner adhesion to paper occurs both mechanically and chemically. As toner penetrates into the voids in paper structure, polymeric molecules interlock within themselves and with the surface. Paper porosity and roughness have pronounced influence on the adhesion, due to better chance of intermingling between the polymer particles, and a greater potential for bonding area. Paper surface energy affects wetting, and is influenced by organic compounds added as internal or surface sizing.

The fixing of toner images may be described in terms of a window, or operating space, which incorporates physical boundaries and process limitations. For hot roll fusing and belts, the window is bounded at high temperature by hot offset or by gloss, and at low temperature, by some minimum fuse quality. Hot offset is a manifestation of failure of the toner to release from the surface of the hot roll, which is influenced by the cohesive strength of the molten toner and adhesion to the roll. Thus, speaking of fix we are looking inside this window of operation and on the material and fuser parameters, which determine the fuse quality.

Toner is typically a blend of amorphous, thermoplastic polymers and other additives. First, the toner is heated to temperatures above its glass transition, typically 60-70°C, where large-scale chain mobility begins, allowing the random particles to become more spherical in shape. The steps of sintering, spreading and penetration take place, followed by cooling of the fused image, which causes the toner to return to the glassy state.

When temperature is increased, print quality improves as judged for example by Taber Abrader and Crease, but not by the same scores. Crease and tape lift-off performance often lag behind abrasion performance. That is, saturation on one scale does not assure satisfactory performance on other merit scale. Abrasion seems to depend on toner cohesion while crease and tape-lift-off appear to be dominated by adhesion forces between paper fibers and toner.

The underlying processes can be elucidated by considering the definitions of fuse and fix. An image may be defined as fused if the molten toner has coalesced, flowed and penetrated into the interstices of paper fibers. An image maybe defined as fixed if its adhesion to paper is sufficiently strong that attempts to physically remove the image will eventually result in removal of paper fibers. From these definitions, Taber Abrader measures the fuse level (degree of coalescence, flow and penetration), whereas crease measures fix (degree of adhesion and area of contact). It is the

degree of completion of the steps involved in fusing and in fixing, that ultimately determines the quality.

Paper Structure

Typically, uncoated paper has *surface* roughness in the micron range, and in the *bulk*, a porosity level in the submicron range. *Toner flow in these two regions is not the same*. Measurements of porosity indicate that if we assume uniform pores then the average pore size for uncoated paper is of the order $r = 0.1\text{-}1\ \mu m$.

Paper consists of a mat of fibers, about *50%* by volume being air. If N is the number of pores per cm^2, then for $r=0.1\ \mu m$, $N = 0.5/\pi r^2 = 1.6\times10^9$ holes/cm². That is, *40000* holes per linear cm or *4* holes per micrometer, so that the distance between pores is *0.05 μm*. If toner penetrates the pores through a uniform distance, *Y*, this translates into an equivalent thickness X absorbed by the paper according to the expression below:

$$X = \pi r^2 Y N = 0.5\,Y$$

On the surface, one may again consider uniform channels, but these formations will be in the micron range, and wetting and free expansion of the toner will be more prominent. In this case, one would expect that adhesion of toner to paper would depend on surface coverage, while in the pore the metric for quality would be depth of penetration.

Channel Flow

Consider the flow in a channel due to a pressure difference across the ends, **Figure 2**. The flow may be described by Equation (1) (Prandtl and Tietjens [1]):

$$\Delta P = \rho U^2 + 8\eta\, l \frac{U}{r^2} \qquad (1)$$

Plots of Equation (1) illustrated in **Figure 3**, show that two distinct modes of flow could occur, viscosity-dominated flow at small values of r and free expansion at large values of r, with abrupt transition in between. The significance of this is that one can treat the flow of the toner on the surface of the paper by the free expansion term, and in the pores, by the viscosity-dominated term.

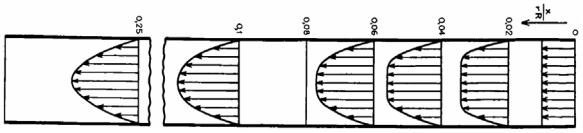

***Figure 2**. Laminar Velocity Distribution in a Channel (Prandtl and Tietjens, [1]*

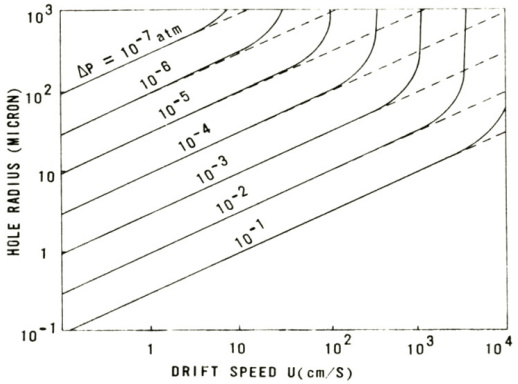

***Figure 3**. Plots of Equation (1) for Flow in a Channel*

Tabor Abrasion Model

Let us assume that image fix, represented by quantity F depends on toner thickness X 'absorbed' into the paper. For $X=0$, $F=0$, and for very large X, F would asymptote to some upper value F_{max}. This behavior may be represented by Equation (2):

$$F(X) = F_{\max}\{1 - \exp(-SX)\} \qquad (2)$$

S is the inverse of some characteristic length, and X is related to toner penetration into paper. Although Equation (2) is arbitrary, it is similar to an empirical relationship that exists between optical density and ink thickness on a substrate. When X is small, the incremental fraction in fix level is linearly proportional to the incremental fraction in toner thickness absorbed, indicating image fix and toner penetration are related, as shown in Equation (3).

$$\frac{\Delta F}{F} = \frac{\Delta X}{X} \qquad (3)$$

Flow in the Pore

Suppose now that paper is a homogeneous medium having cylindrical pores of radius r, running in parallel across the thickness of the sheet. The contact pressure forces toner into the pore capillaries generating a Poiseuille flow represented by the viscous term in Equation (1), with a strong dependence on pore radius, as shown in **Figure 4**.

For an advancing interface

$$l \approx y,\ U \approx \frac{dy}{dt},\ \Delta P \approx P$$

This yields Equation (4):

$$P = 8\eta(T)\frac{y}{r^2}\frac{dy}{dt} \qquad (4)$$

Here P is contact pressure, y penetration at time t, r the pore radius and η toner viscosity at time t.

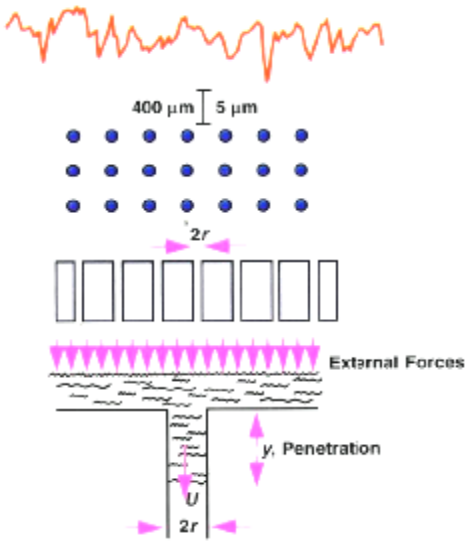

Figure 4. *Model Structure of Paper Showing Surface Roughness, Hypothesized Parallel Channels, and Flow in the Pore*

The viscosity is a function of temperature, defined here by the Arrhenius relationship given in Equation (5).

$$\eta(T) = \eta_r \, Exp\left\{\frac{E_a}{R}\left(\frac{1}{T} - \frac{1}{T_r}\right)\right\} \qquad (5)$$

η_r is a reference value, E_a is the activation energy of viscosity - temperature curve of the toner, and R the gas constant. Since temperature is a function of distance and time, viscosity will also vary with time, and this dependence has to be determined to integrate Equation (4).

For a belt-fusing system, heat flows from the belt to the image as well as from the backup roll to the paper. In the present case, the thermal properties of the various layers are comparable; for simplicity, one medium is assumed throughout, as described below.

- Thermal Conductivity, W/m/°C: $k = 0.3$
- Thermal diffusivity, cm²/sec: $\alpha = 0.002$
- Thickness, µm: $h = 380$

The heat transfer model described in **Figure 5** and (Equation (6)) below addresses the thermal problem of the belt. A thickness h representing the belt, enters the nip at temperature T_R, this meets a layer of thickness s representing toner and paper that are initially at ambient temperature T_A, and bounded by a backup roll at temperature T_B, for duration of the dwell t_d in the nip. The inner interface at $x = -h$ remains at constant temperature, T_R.

The solution for the temperature profile $T(x,t)$ as a function of distance and time is given in Equation (6) (Carslaw and Jaeger [2]).

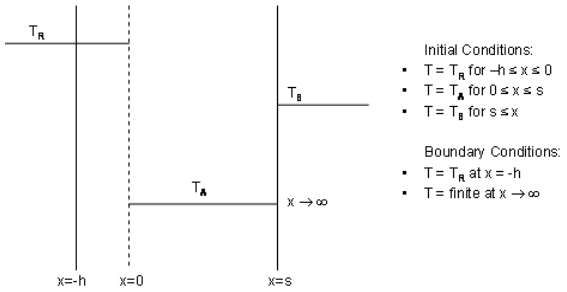

Figure 5*. Heating of a Semi-infinite Homogeneous Medium*

$$\frac{T_R - T(x,t)}{T_R - T_A} = \frac{1}{2}\left[\begin{array}{l} erf\left\{\dfrac{x}{\sqrt{4\alpha t}}\right\} + erf\left\{\dfrac{x+2h}{\sqrt{4\alpha t}}\right\} - \dfrac{T_B - T_A}{T_R - T_A} \times \\ \left(erf\left\{\dfrac{x-s}{\sqrt{4\alpha t}}\right\} + erf\left\{\dfrac{x+2h+s}{\sqrt{4\alpha t}}\right\}\right) \end{array}\right] \qquad (6)$$

Penetration Equation

Equation (4) may be integrated using Equation (5) and Equation (6), as shown in Equation (7):

$$\int_0^Y y\,dy = \frac{\Pr^2}{8}\int_0^{t_d} \frac{dt}{\eta(T(x,t))} \qquad (7)$$

By introducing the assumption of small perturbations, an intermediate step in the analysis yields Equation (8) for the penetration of the toner at distance x_t at the end of the dwell t_d:

$$Y^2 = \frac{P t_d r^2}{4\eta(T_{nip})}\int_0^1 \exp\left[-\varepsilon^{-1} erf\left\{(\tau\theta)^{-1/2}\right\} + \varepsilon'^{-1}\left(1 + erf\left(\tau'\theta\right)^{-1/2}\right)\right] d\theta$$

$$\tau = 4\alpha\frac{t_d}{x_t^2}; \quad \tau' = 4\alpha\frac{t_d}{(x_t - s)^2}; \quad T_{nip} = \frac{1}{2}(T_R - T_A) + T_A(^\circ K) \qquad (8)$$

ε, ε' are constants of the configuration, typically *0.1-0.2.*

Further simplifications can be carried out to integrate Equation (8) above, and achieve the master relationship Equation (9) for the belt temperature in terms of the penetration, Y:

$$\frac{T_R - T_A}{T_r - T_A} = \left\{\left(\frac{P t_d r^2}{4\eta_r Y^2}\right)^{-\varepsilon} + \frac{2}{\sqrt{\pi\alpha t_d}}\left[x_t + \frac{T_B - T_A}{T_r - T_A}(s - x_t)\right]\right\} \times$$

$$Exp\left(-\frac{T_B - T_A}{T_r - T_A}\right); \quad \varepsilon^{-1} = \frac{E_a / R}{\left[T_A(^\circ K) + \dfrac{T_r - T_A}{2}\right]^2} \times \frac{(T_r - T_A)}{2} \qquad (9)$$

ε is related to the activation energy and reference temperature of the toner

Equation (9) expresses the belt temperature T_R required to achieve a given fix level Y for a specific fusing configuration (e.g., hardware, materials). Alternatively, given a particular fuse grade, one can determine the belt temperature. The relationship shows the

effects of pressure P and dwell t_d, and also of toner pile height x_t, media thickness s, and backup roll temperature T_B.

Constant Fix Criterion

Of particular interest are the conditions for constant fix level, that is, the trade-offs that can be used to obtain constant image fix. For two fusing configurations the condition for constant fix demands that the penetration be the same, Equation (10):

$$Y = Y_o \tag{10}$$

By applying Equation (9) for two cases with the same penetration, and after some manipulation, we obtain the fusing temperature of the belt required to achieve constant image fix. This is shown in Equation (11):

$$\frac{T_R - T_A}{T_{Ro} - T_A} = \left[\begin{array}{l} \left(\frac{P t_d r^2 / \eta_r}{P_o t_{do} r_o^2 / \eta_{ro}} \right)^{-\varepsilon} + \frac{2}{\sqrt{\pi\alpha}} \left(\frac{x_t}{\sqrt{t_d}} - \frac{x_{to}}{\sqrt{t_{do}}} \right) + \\ \frac{2}{\sqrt{\pi\alpha}} \frac{T_{Bo} - T_A}{T_{Ro} - T_A} \left(\frac{(s - x_t)}{\sqrt{t_d}} - \frac{(s_o - x_{to})}{\sqrt{t_{do}}} \right) - \frac{T_B - T_{Bo}}{T_{Ro} - T_A} \end{array} \right] \tag{11}$$

T_R	Belt fusing temperature
P	Nip pressure
t_d	Dwell time
T_A	Paper initial temperature
T_B	Backup roll temperature
ε	Constant defined by Equation (9)
η_r	Reference viscosity at temperature and shear rate
r	Mean pore size of paper
s	Paper thickness
x_t	Pile height of toner
o	Subscript denoting reference value, e.g., T_{Ro}

The first term on the r.h.s. of Equation (11) involves the effect of pressure, dwell, toner viscosity and paper pores. The second term describes the effect of toner pile height and its sensitivity to thermal diffusion. The third term involves the effect of paper thickness, and the fourth term describes the effect of the backup roll temperature. It can be also shown that if paper is preheated and its temperature is different from the ambient temperature, Equation (11) will involve an additional term similar to the forth term on the r.h.s.

In conclusion, the results indicate that *fix is enhanced by increases in the following parameters: belt temperature, dwell, pressure at the nip; porosity; backup roll temperature, and paper preheating. Fix degrades as increases occur in toner viscosity, toner pile height, and media thickness. The above trends seem to be in agreement with expectations.*

Crease Analysis

Image crease modeling is carried out using the inertia-driven component of flow in a channel (Equation (1)), where the pattern is more characteristic of the coalescence and spreading phase of the process. **Figure 6** is a schematic representation of the flow pattern configuration for crease.

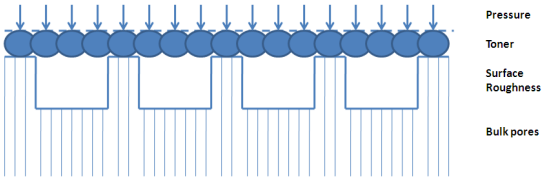

***Figure 6**. Paper Structure Model for Crease Analysis*

For an advancing flow, Equation (12) is obtained:

$$P = \rho(T) \left(\frac{dz}{dt} \right)^2 \tag{12}$$

The density, ρ, is not a constant but rather a function of temperature and time, as toner particles coalesce and voids merge. Thus, density maybe defined by the Arrhenius relationship below:

$$\rho(T) = \rho_{nip} \; Exp\left[\frac{E_c}{R} \left\{ \frac{1}{T(x,t)} - \frac{1}{T_{nip}} \right\} \right] \tag{13}$$

Integration of Equation (12) yields Equation (14), where Z is the extent of the flow into the surface of the paper after duration t_d of the dwell:

$$Z = \int_0^Z dz = \sqrt{P} \int_0^{t_d} \frac{dt}{\sqrt{\rho(T)}} \tag{14}$$

The metric for crease, Γ, may be defined as the area wetted by the advancing flow and in particular, by the wetted area for the specific cross section, as shown in Equation (15). Here, D is of the order of the diameter of toner particle, as the relevant paper roughness for this type of flow cannot be smaller than the particle size.

$$\Gamma = \frac{\pi D \times Z}{\pi D^2 / 4} \approx \frac{Z}{D} \tag{15}$$

This expression shows that the metric for crease is highest for roughness level comparable to toner particle size. In such cases, adhesion is maximized. For roughness that is much larger than the diameter, D, the contribution to adhesion would be negligible.

The temperature profile through the layers is given by Equation (6). Keeping the analysis to first-order terms as with abrasion, one may derive an expression relating the belt temperature to the crease level, as shown in Equation (16):

$$\frac{T_R - T_A}{T_r - T_A} = \left\{ \begin{array}{l} \left(\frac{4P t_d^2}{\Gamma M D} \right)^{-\varepsilon_c} + \frac{4}{\sqrt{\pi\alpha}} \left(\frac{x_t}{\sqrt{t_d}} \right) + \\ \frac{T_B - T_A}{T_r - T_A} \frac{4}{\sqrt{\pi\alpha}} \frac{(s - x_t)}{\sqrt{t_d}} \end{array} \right\} Exp(-2 \frac{T_B - T_A}{T_r - T_A}) \tag{16}$$

Constant crease criterion for two fusing configurations, i.e., $\Gamma=\Gamma_o$, may be expressed explicitly as shown in Equation (17):

$$\frac{T_R-T_A}{T_{Ro}-T_A}=\left[\begin{array}{l}\left(\frac{Pt_d^2/(MD)}{P_o t_{do}/(M_o D_o)}\right)^{-\varepsilon_c}+\frac{4}{\sqrt{\pi\alpha}}\left(\frac{x_t}{\sqrt{t_d}}-\frac{x_{to}}{\sqrt{t_{do}}}\right)+\\ \frac{4}{\sqrt{\pi\alpha}}\frac{T_{Bo}-T_A}{T_{Ro}-T_A}\left(\frac{(s-x_t)}{\sqrt{t_d}}-\frac{(s_o-x_{to})}{\sqrt{t_{do}}}\right)-2\frac{T_B-T_{Bo}}{T_{Ro}-T_A}\end{array}\right] \quad (17)$$

In Equations (16) and (17), ε_c has an expression similar to ε (Equation (9)), except that activation energy (E_a) is replaced by coalescence and spreading energy (E_c); D is toner particle diameter; M is toner mass per unit area.

Equation (16) shows that crease performance improves as surface temperature, T_R, goes up, as the ratio Pt^2/MD increases, as pile height to dwell time ratio $x_t/\sqrt{\alpha t_d}$ goes down, and as thermal properties of fusing surface increase. The index ε_c is a small quantity ~ *0.1* which depends on parameters such as activation energy of the density-temperature relationship of the coalescence spreading process, and others.

Discussion

Measurements by Prime [3] show that abrasion merit exhibits a dependence on the product Pt, whereas scratch data show a dependence on Pt^2. Britto [4] made a parametric analysis of abrasion phenomenon and identified two dimensionless parameters relevant to fixing quality, namely Pt/η and $\alpha t/L^2$. Chen and Yang [5] carried-out dimensional analysis of factors affecting fusing quality, by conducting adhesive tape peeling test, and using the ratio of optical density before and after tape peel-off as criterion. The authors obtained two dimensionless parameters affecting quality, namely Pt^2/MD and T/T_A. All these observations are in agreement with predictions from Equations (9) and (16). Furthermore, the two master relationships show explicitly the effects of media thickness, backup roll temperature, and thermal properties of the system, all relative to the temperature required of the belt or fusing surface to achieve a given level of fix. The conclusion is that the metrics used to characterize abrasion and crease, based on channel flow, seem to be meaningful and represent the mechanisms involved in the processes. The crease metric $\Gamma = Z/D$ suggests that the toner particles should be made small; it also suggests that paper roughness should match the toner particle size for crease performance. Wetting thickness, Z, increases with pressure and with the square of the dwell, while keeping toner mass per unit area at a low level that is still compatible with the optical density.

Equations (10) and (17) are particularly useful for designing the fusing process for a given configuration, for identifying the trade-offs relative to hardware and material selection, and for scoping sensitivities to changes in process and loading conditions. *Once the belt temperature is known, one can calculate the heater temperature and fusing power requirements of the system.*

Examples of sensitivities of belt temperature to changes in process parameters to maintain constant abrasion fix level are listed below:

- ppm from 25 to 40 $\Delta T_R = +15°C$
- Load from 40# to 60# $\Delta T_R = -9.2°C$
- Pile height from 10µm to 15µm $\Delta T_R = +9.8°C$
- BUR temp. from 80°C to 90°C $\Delta T_R = -9.6°C$
- Media from 90gsm to 105gsm $\Delta T_R = +10.9°C$

Figure 7 illustrates an example of how the fix model can be used to design the fusing process and choose hardware. For a high speed scenario, a domain of load versus rubber thickness required to achieve a given fix level is depicted, and various curves are shown for life, belt temperature, pressure, and so forth. This integrated approach helps to identify an optimum domain where the spec on the subsystem is satisfied.

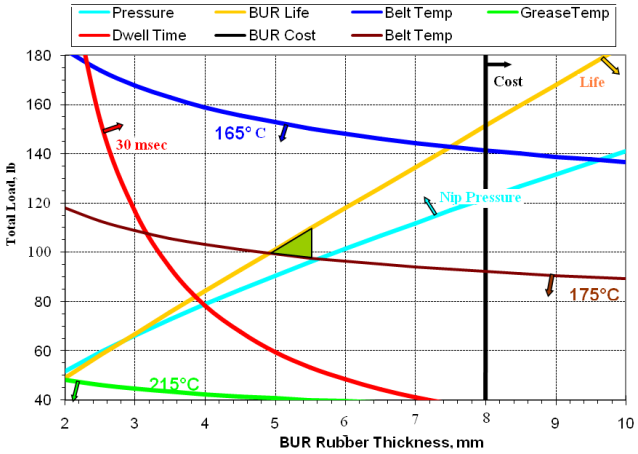

Figure 7. Example of Fusing Process Optimization at High ppm

REFERENCES

[1] Prandtl, L. & Tietjens, O.G., "Applied Hydro- and Aeromechanics", Dover Publications, New York, p.24 (1934).

[2] Carslaw, H.S. and Jaeger, J.C., "Conduction of Heat in Solids" Oxford University Press (1959).

[3] Prime, R.B., "Relationship Between Toner Properties, Fuser Parameters, and Fixing of Electrographic Images", Photo. Sci. and Eng., Vol.27, pp.19-25 (1983).

[4] Britto, I.L., "An Evaluation of Factors that Control the Fixing of Toner to Paper in Laser-Printing", Proceedings of IS&T's 7th International Congress on Advances in Non-impact Printing Technologies, Vol.1, pp.386-400 (1991).

[5] Chih-Hung Chen & Tsai-Bou Yang, "Dimensional Analysis on Toner fusing Process", Recent Progress in Toner Technologies, pp.401-403 (1997).

Author Biography

David Battat received his DPhil in Engineering Science from Oxford University. England. He was Principal Scientist with Xerox Corporation in Webster, NY. He has worked with Lexmark International in Lexington, KY since 2007.